

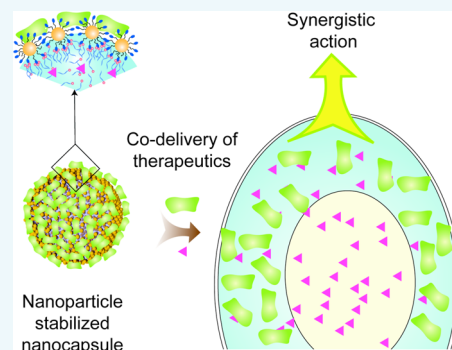
# Co-Delivery of Protein and Small Molecule Therapeutics Using Nanoparticle-Stabilized Nanocapsules

Chang Soo Kim, Rubul Mout, Yunlong Zhao, Yi-Cheun Yeh, Rui Tang, Youngdo Jeong, Bradley Duncan, Jeanne A. Hardy, and Vincent M. Rotello\*

Department of Chemistry, University of Massachusetts, 710 North Pleasant Street, Amherst, Massachusetts 01003, United States

## S Supporting Information

**ABSTRACT:** Combination therapy employing proteins and small molecules provides access to synergistic treatment strategies. Co-delivery of these two payloads is challenging due to the divergent physicochemical properties of small molecule and protein cargos. Nanoparticle-stabilized nanocapsules (NPSCs) are promising for combination treatment strategies since they have the potential to deliver small molecule drugs and proteins simultaneously into the cytosol. In this study, we loaded paclitaxel into the hydrophobic core of the NPSC and self-assembled caspase-3 and nanoparticles on the capsule surface. The resulting combination NPSCs showed higher cytotoxicity than either of the single agent NPSCs, with synergistic action established using combination index values.



## INTRODUCTION

Combination therapies provide the potential for increased efficacy through synergies between therapeutics.<sup>1–4</sup> For example, co-delivery of siRNA and small molecule drugs can be used to reduce drug administrations through knockdown of multidrug resistance.<sup>5–7</sup> Simultaneous delivery of small molecule drugs and proteins likewise provides a promising therapeutic strategy that has been employed in cancer therapy<sup>8,9</sup> and immunotherapy.<sup>10</sup> One key challenge for protein–drug co-delivery is the distinct properties required for encapsulation of small drugs, often hydrophobic, and large hydrophilic proteins that are sensitive to environmental unfolding and irreversible denaturation. Beyond simple delivery, a second key challenge is that delivered proteins are often entrapped within endosomes and consequently degraded in lysosomes, resulting in very low therapeutic efficacy.<sup>11–13</sup>

In recent research, we have shown that nanoparticle-stabilized capsules (NPSCs) can be used to deliver small molecules to cells,<sup>14</sup> and proteins directly to the cytosol.<sup>15</sup> We hypothesized that these two delivery modalities could be combined to generate useful combination therapeutic delivery systems. Our system was designed to prevent cell division, which would limit tumor growth, and concurrently induce apoptotic cell death. To this end we self-assembled the apoptosis-inducing protein caspase-3 (CASP3)<sup>16,17</sup> and gold nanoparticles (AuNPs) on the surface of a fatty acid droplet containing paclitaxel (PTX),<sup>14</sup> a known inhibitor of mitotic spindle assembly that prevents cell division (Figure 1). The resulting NPSCs successfully induced cell death and in addition demonstrated pharmacological synergy, as established through Chou-Talalay analysis.<sup>18</sup>

## RESULTS AND DISCUSSION

We have developed a method that allowed production of stable NPSCs containing both CASP3 and PTX in just three steps (Figure 1, Supporting Information).<sup>14,15</sup> First, PTX (LogP 3.54, MW 854) was dissolved in linoleic acid (10 mg/mL). An emulsion was then formed from this solution using a commercial amalgamator. Gold nanoparticles functionalized with arginine ligands (Arg-AuNPs) were then assembled on the surface through electrostatic attractions<sup>19</sup> (Table S1, Figure S1). After NPSC stabilization, negatively charged proteins were incorporated into the NPSC shells. In these studies, transferrin (TF, pI = 5.6, monomer MW = 76 kDa)<sup>14</sup> and CASP3 (pI = 6.7, heterotetramer, total MW = 59.2 kDa) were used as a control and a therapeutic protein, respectively.

NPSC size was established using dynamic light scattering (DLS) and transmission electron microscopy (TEM) (Table S2, Figure S2), and characterized by zeta potential measurements (Table S2). In general, the size of NPSCs increased only modestly after protein incorporation (Figure 2C, Table S2), as would be expected from the addition of proteins via charge-mediated adduction. After optimization, NPSCs of 130–140 nm (diameter) were produced. TEM images of NPSCs showed packing of nanoparticles, and efficient assembly, as no significant amount of free nanoparticle was observed on the rest of the TEM sample grid (Figures 2B and S2). TEM micrographs of NPSC–CASP3 stained by uranyl acetate showed the shell the structure of proteins around the NPSC, confirming

Received: March 19, 2015

Revised: April 15, 2015

Published: April 20, 2015

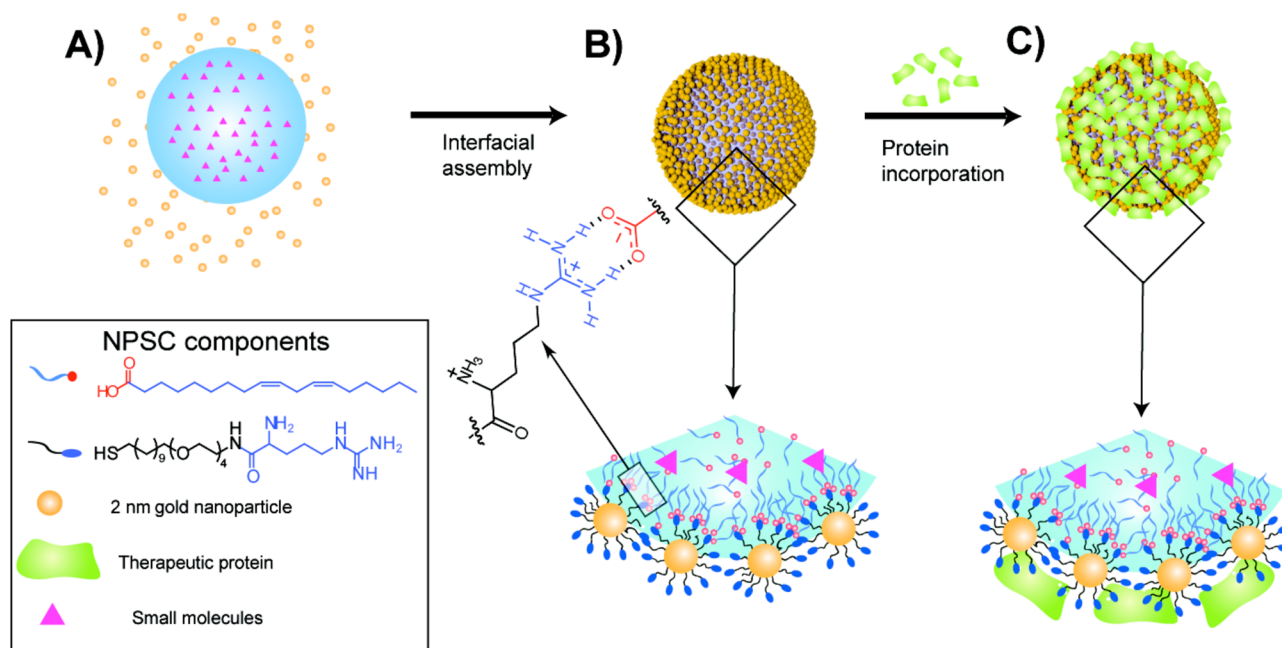


**Figure 1.** NPSC fabrication. (A) Template droplets (with or without PTX) were generated using an amalgamator. (B) Droplets were transferred to Arg-AuNP solution to generate NPSCs. (C) Incorporation of CASP3 or transferrin (control) onto the NPSC surface.

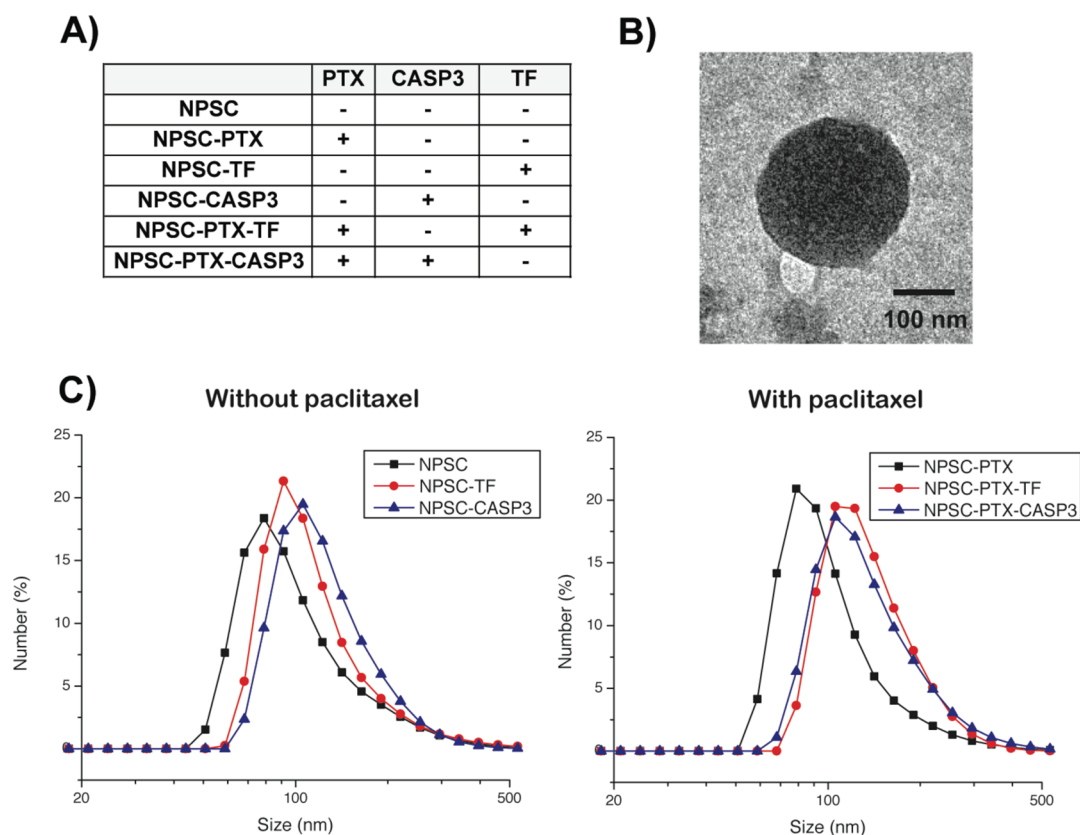


**Figure 2.** Characterization of NPSCs. (A) NPSCs used in these studies. (B) TEM micrograph of NPSC-PTX-CASP3. (C) Hydrodynamic diameters of NPSCs as measured by DLS before and after protein inclusion, showing modest increase in size.

the successful integration of protein onto the NPSC surface (Figure S3).

The dual-cargo NPSCs were designed to inhibit cell growth and induce apoptotic death. To measure the apoptotic potential of the NPSCs, we incubated NPSCs with HeLa cells. After a 1-h incubation period, the cells were treated simultaneously with

the general apoptotic marker, Yopro-1 (green) and with the late apoptotic marker 7-AAD (red).<sup>15</sup> The HeLa cells were observed after 30 min of treatment with a fluorescence microscope (Figure 3). The quantification of fluorescence images showed that  $97 \pm 2\%$  of HeLa cells treated with NPSC-PTX-CASP3 were apoptotic (Figure 3B), far higher than TF-

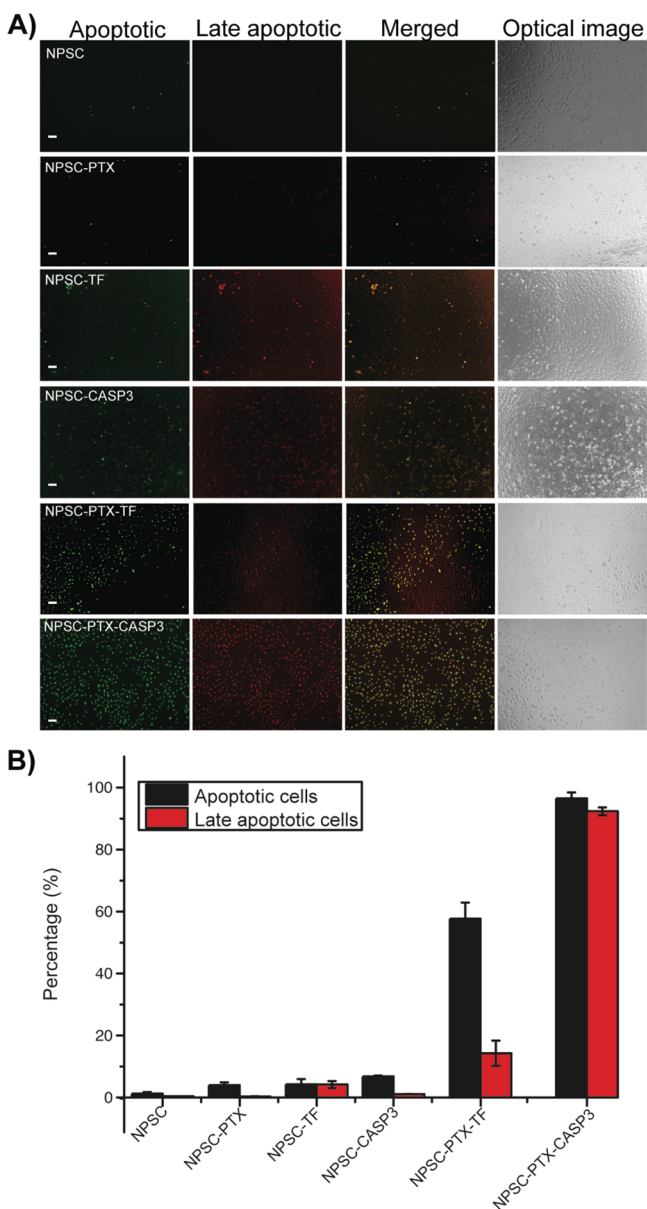


**Figure 3.** Co-delivery of CASP3 and PTX into HeLa cells. (A) Apoptotic (Yopro-1, green fluorescence) and late apoptotic cells (7-AAD, red fluorescence) were observed after 1-h incubation with different NPSCs in serum free DMEM. Scale bar: 500  $\mu$ m. (B) Quantification of the apoptosis percentage.

coated control (NPSC-PTX-TF,  $58 \pm 5\%$ ) or paclitaxel-free control (NPSC-CASP3,  $7 \pm 0.3\%$ , Figure 3B). The fluorescence images of cells treated with NPSC-PTX-CASP3 showed  $92 \pm 1\%$  of late apoptotic HeLa cells with membrane disruption, compared to the control group, NPSC-PTX-TF ( $14 \pm 4\%$  of membrane disruption), indicating the importance of CASP3 for entry into apoptosis.

We next measured cell viabilities using an Alamar blue assay. No significant cell death was observed from the individual components (Arg-AuNP, CASP3, and TF only, Figure S4). Further, NPSC and NPSC-TF did not show any substantial cell killing ability (Figure 4). PTX-loaded NPSCs (NPSC-PTX, NPSC-PTX-TF, and NPSC-PTX-CASP3) and CASP3-stabilized NPSCs (NPSC-CASP3 and NPSC-PTX-CASP3) showed concentration-dependent cell death (Figure 4). Consistent with the apoptosis study, the highest rates of killing were observed

with NPSC-PTX-CASP3 ( $57 \pm 0.7\%$  cell viability at 6 pM of nanocapsule concentration), indicating either a synergistic or additive effect of the dual payload.

To evaluate possible synergy between PTX and CASP3, we used the Chou–Talalay method to evaluate the synergies present in the dose–response analysis.<sup>18</sup> The Chou–Talalay analysis is widely used to determine whether two effects are synergistic or additive by calculating combination index (CI) values. CI values quantitatively depict synergism ( $CI < 1$ ), additive effect ( $CI = 1$ ), or antagonism ( $CI > 1$ ).<sup>20</sup> In these studies, the CalcuSyn algorithm (Biosoft, Cambridge, UK) was used to calculate CI values. Additionally, CI values at  $ED_{50}$  and  $ED_{75}$  (effective dose leading to a 50% or 75% response) were measured.<sup>21</sup> Based on the combination index table<sup>22</sup> (Figure 4B), very strong synergistic effects were observed with NPSC-PTX-CASP3 at low doses. Also, the CI values of  $ED_{50}$  and  $ED_{75}$  were 0.24 and 0.70, respectively, representing an overall synergism ( $CI < 0.7$ ) from the combined therapy.

To gain a better understanding of the efficacy of the capsules, we extended the incubation time with the NPSCs to 20 h. HeLa cells were incubated with NPSCs in DMEM media containing 10% fetal bovine serum (FBS). Consistent with 1-h incubation results, the highest rates of cell death were observed with NPSC-PTX-CASP3 ( $26 \pm 0.4\%$  viability at 12 pM NPSC concentration, Figure 5). Other control groups showed reduced efficacy (NPSC-CASP3,  $33 \pm 0.1\%$ ; and NPSC-PTX-TF,  $42 \pm 0.6\%$ ; Figure 5). Strong synergistic effect ( $CI < 0.3$ ) with extended incubation time (20 h) was observed with NPSC-PTX-CASP3 at lower doses (Figure 5B). Also, CI values of  $ED_{50}$  and  $ED_{75}$  were 0.25 and 0.30, respectively, representing stronger overall synergism ( $CI < 0.3$ ) from the extended incubation time (20 h) than the 1-h incubation ( $CI < 0.7$ ).

## CONCLUSIONS

In summary, we have developed a series of NPSC that allow packaging both proteins and small molecule drugs without leakage of the small molecules or entanglement and denaturation of the proteins. These NPSCs are efficient at simultaneous co-delivery of an antimetabolic small molecule drug and a proapoptotic protein into cell cytosol. We observed enhanced efficacy using this dual delivery approach, providing a potential strategy for next-generation therapies that integrate the activities of proteins and small molecule therapeutics. Due to the design of our NPSC, we foresee that this strategy should be applicable to nearly any small molecule, regardless of LogP and proteins of a wide range of molecular weights.

## EXPERIMENTAL PROCEDURES

**Materials.** All the chemicals were purchased from Sigma-Aldrich or Fisher Scientific, unless otherwise specified. Paclitaxel was purchased from LC Laboratory. Chloroauric acid was bought from Strem Chemicals Inc. (Newburyport, MA).

**Arginine Functionalized Gold Nanoparticle (Arg-AuNP) Synthesis.** Gold nanoparticles (AuNPs) protected with 1-pentanethiol (C5) and arginine-terminated thiol ligands were prepared following the reported procedure.<sup>23,24</sup> Briefly, 10 mg of C5-protected AuNPs were first dissolved in 1 mL of dry dichloromethane (DCM). Arginine-terminated thiol ligands (40 mg) were dissolved in 5 mL of organic solvent (DCM: MeOH = 4:1 v/v), and then added to the solution of C5-protected AuNPs. The reaction mixture was stirred at room

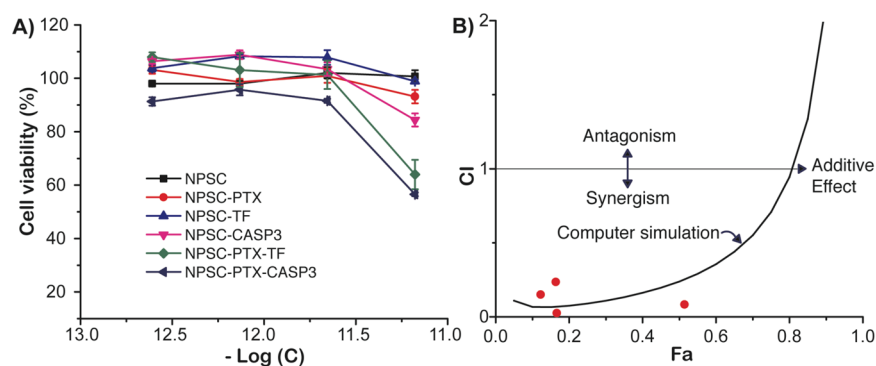


**Figure 4.** Cell viability measurement and synergy calculation after 1-h incubation with different NPSCs in serum-free DMEM. (A) Cell viability as a function of nanocapsule concentration (C) was measured using an Alamar blue assay. (B) Combination index (CI) values were calculated by Chou–Talalay analysis of the Fraction affected (Fa). Red dots are data from NPSC-PTX-CASP3 viability.

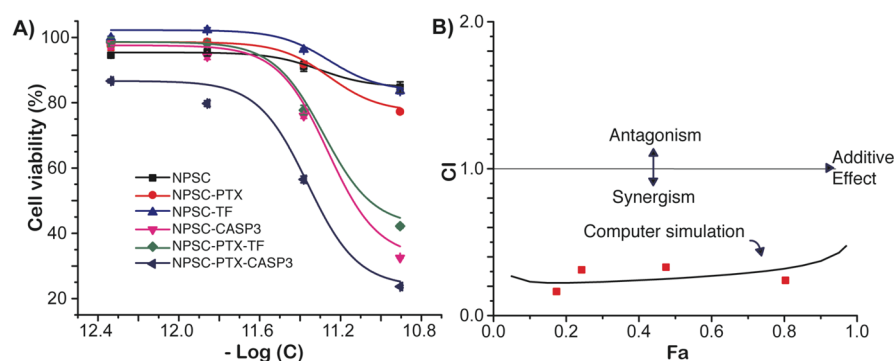


**Figure 5.** (A) Cell viability after 20-h incubation in DMEM media containing 10% serum as a function of Nanocapsule concentration (C). (B) CI plot calculated by Chou–Talalay analysis. Red dots are observed combination data points after NPSC-PTX-CASP3 treatment.

temperature for 3 days. Finally, the organic solvent was evaporated and Arg-AuNPs were dissolved in Milli-Q water. The aqueous solution of Arg-AuNP was purified by dialysis for 3 days. The hydrodynamic size and zeta potential of Arg-AuNP were measured by DLS (Table S1). Also, the TEM image confirmed the homogeneous Arg-AuNP with a 2-nm-diameter core size (Figure S1).

**NPSC Formation.** NPSCs with different proteins were fabricated by following our previous literature with slight modifications.<sup>14</sup> Briefly, template droplets were generated by agitating 1  $\mu$ L of linoleic acid in 485  $\mu$ L of a phosphate buffer (5 mM, pH 7.4) in 14  $\mu$ L of Arg-AuNP (37  $\mu$ M) using an amalgamator (YDM-Pro, Yinya New Materials Co. Ltd., Hangzhou, China) at 5000 rpm for 100 s. NPSCs containing paclitaxel were synthesized by using the same template droplet procedure, but using paclitaxel dissolved (10 mg/mL) linoleic acid. The template droplets (20  $\mu$ L) were added to 5  $\mu$ L of Arg-AuNP solution (37  $\mu$ M) in 72  $\mu$ L of a phosphate buffer (5 mM, pH 7.4) and mixed to form NPSCs. After 10 min of stabilization, 97  $\mu$ L of NPSCs were mixed with 3  $\mu$ L of proteins (20  $\mu$ M), such as caspase-3 and transferrin. The formed NPSCs were then directly used for characterization and cell culture applications.

**NPSC Characterization.** The sizes of NPSCs with different proteins were characterized by DLS and TEM. The size measurements with DLS were performed by using a Malvern Zetasizer (Nano series, Malvern Instruments Inc., USA). The TEM samples of NPSCs with different proteins were prepared by a drop-casting method onto a 300-mesh nickel grid coated with Formvar film. The TEM images of samples were measured by using a JEOL 200FX transmission electron microscope.

Also, the electrical charges (zeta potentials) of NPSCs with different proteins were measured by a particle electrophoresis instrument using a Malvern Zetasizer. The concentration of NPSCs was calculated according to a reported method.<sup>14</sup>

**Cell Viability (Alamar Blue Assays).** HeLa cells were cultured at 37 °C under a humidified atmosphere of 5% CO<sub>2</sub>. The HeLa cells were grown in a low-glucose Dulbecco's modified Eagle's medium (DMEM, 1.0 g/L glucose) containing 10% fetal bovine serum (FBS) and 1% antibiotic (100 U/mL penicillin and 100  $\mu$ g/mL streptomycin). The HeLa cells were maintained in the above medium and subcultured once every 4 days. The HeLa cells ( $6 \times 10^4$  cells/well) were seeded in a 24-well plate 24 h prior to delivery. On the next day, the old media was removed and the cells were washed with a phosphate buffer saline (PBS) three times before NPSC delivery. The cell viability was measured using an Alamar Blue assay (Invitrogen, CA).

**Apoptosis and Membrane Disruption Studies.** For the apoptosis and membrane disruption studies, we followed our previous staining, imaging, and quantification methods.<sup>15</sup> HeLa cells ( $6 \times 10^4$  cells/well) were seeded in a 24-well plate 24 h prior to delivery. On the next day, the old media was removed and the cells were washed with a PBS three times before NPSC delivery. After the NPSC delivery (10.3  $\mu$ M), the cells were stained by Yopro-1 (a dye to detect apoptotic cell nuclei) and 7-AAD (a dye used to detect late apoptotic cells by membrane disruption) for 30 min. Then, the stained cells were observed under a fluorescence microscope (Olympus IX61, Japan) and the fluorescent images were quantified by *ImageJ* using a cell counter method.

**Statistical Analysis.** The synergy of co-delivery of therapeutics was analyzed using a median-effect analysis as originally described by Chou and Talalay.<sup>18</sup> Combination indexes (CIs) for NPSCs were generated with the CalcuSyn algorithm (Biosoft, Cambridge, UK). CIs determined the combination effect as synergistic (<1), additive (=1), or antagonistic (>1). Also, 50% and 75% effective doses (ED) were reported for each analysis.

## ■ ASSOCIATED CONTENT

### 📄 Supporting Information

Caspase-3 expression and purification; characterization of nanoparticle, nanocapsules, and caspase-3; control cell viability experiment. This material is available free of charge via the Internet at <http://pubs.acs.org>.

## ■ AUTHOR INFORMATION

### Corresponding Author

\*E-mail: [rotello@chem.umass.edu](mailto:rotello@chem.umass.edu). Phone: +1-413-545-2058. Fax: +1-413-545-4490.

### Notes

The authors declare no competing financial interest.

## ■ ACKNOWLEDGMENTS

This research was supported by the NIH (EB014277).

## ■ REFERENCES

- (1) Peer, D., Karp, J. M., Hong, S., Farokhzad, O. C., Margalit, R., and Langer, R. (2007) Nanocarriers as an emerging platform for cancer therapy. *Nat. Nanotechnol.* 2, 751–760.
- (2) Lehar, J., Krueger, A. S., Avery, W., Heilbut, A. M., Johansen, L. M., Price, E. R., Rickles, R. J., Short, G. F., 3rd, Staunton, J. E., Jin, X., et al. (2009) Synergistic drug combinations tend to improve therapeutically relevant selectivity. *Nat. Biotechnol.* 27, 659–666.
- (3) Lane, D. (2006) Designer combination therapy for cancer. *Nat. Biotechnol.* 24, 163–164.
- (4) Sun, T. M., Du, J. Z., Yao, Y. D., Mao, C. Q., Dou, S., Huang, S. Y., Zhang, P. Z., Leong, K. W., Song, E. W., and Wang, J. (2011) Simultaneous delivery of siRNA and paclitaxel via a "two-in-one" micelle promotes synergistic tumor suppression. *ACS Nano* 5, 1483–1494.
- (5) Zhu, C., Jung, S., Luo, S., Meng, F., Zhu, X., Park, T. G., and Zhong, Z. (2010) Co-delivery of siRNA and paclitaxel into cancer cells by biodegradable cationic micelles based on PDMAEMA-PCL-PDMAEMA triblock copolymers. *Biomaterials* 31, 2408–2416.
- (6) Jhaveri, A., Deshpande, P., and Torchilin, V. (2014) Stimuli-sensitive nanopreparations for combination cancer therapy. *J. Controlled Release* 190, 352–370.
- (7) Saad, M., Garbuzenko, O. B., and Minko, T. (2008) Co-delivery of siRNA and an anticancer drug for treatment of multidrug-resistant cancer. *Nanomedicine (London)* 3, 761–776.
- (8) Lee, A. L. Z., Dhillon, S. H. K., Wang, Y., Pervaiz, S., Fan, W., and Yang, Y. Y. (2011) Synergistic anti-cancer effects via co-delivery of TNF-related apoptosis-inducing ligand (TRAIL/Apo2L) and doxorubicin using micellar nanoparticles. *Mol. Biosyst.* 7, 1512–1522.
- (9) Jiang, T., Mo, R., Bellotti, A., Zhou, J., and Gu, Z. (2014) Gel-liposome-mediated co-delivery of anticancer membrane-associated proteins and small-molecule drugs for enhanced therapeutic efficacy. *Adv. Funct. Mater.* 24, 2295–2304.
- (10) Park, J., Wrzesinski, S. H., Stern, E., Look, M., Criscione, J., Ragheb, R., Jay, S. M., Demento, S. L., Agawu, A., Licona Limon, P., et al. (2012) Combination delivery of TGF-beta inhibitor and IL-2 by nanoscale liposomal polymeric gels enhances tumour immunotherapy. *Nat. Mater.* 11, 895–905.

(11) Kaczmarczyk, S. J., Sitaraman, K., Young, H. A., Hughes, S. H., and Chatterjee, D. K. (2011) Protein delivery using engineered virus-like particles. *Proc. Natl. Acad. Sci. U.S.A.* 108, 16998–17003.

(12) Bale, S. S., Kwon, S. J., Shah, D. A., Banerjee, A., Dordick, J. S., and Kane, R. S. (2010) Nanoparticle-mediated cytoplasmic delivery of proteins to target cellular machinery. *ACS Nano* 4, 1493–1500.

(13) Fu, A., Tang, R., Hardie, J., Farkas, M. E., and Rotello, V. M. (2014) Promises and pitfalls of intracellular delivery of proteins. *Bioconjugate Chem.* 25, 1602–1608.

(14) Yang, X. C., Samanta, B., Agasti, S. S., Jeong, Y., Zhu, Z. J., Rana, S., Miranda, O. R., and Rotello, V. M. (2011) Drug delivery using nanoparticle-stabilized nanocapsules. *Angew. Chem., Int. Ed.* 50, 477–481.

(15) Tang, R., Kim, C. S., Solfiell, D. J., Rana, S., Mout, R., Velazquez-Delgado, E. M., Chompoosor, A., Jeong, Y., Yan, B., Zhu, Z. J., et al. (2013) Direct delivery of functional proteins and enzymes to the cytosol using nanoparticle-stabilized nanocapsules. *ACS Nano* 7, 6667–6673.

(16) Zhao, M., Biswas, A., Hu, B., Joo, K. I., Wang, P., Gu, Z., and Tang, Y. (2011) Redox-responsive nanocapsules for intracellular protein delivery. *Biomaterials* 32, 5223–5230.

(17) Yan, M., Du, J., Gu, Z., Liang, M., Hu, Y., Zhang, W., Priceman, S., Wu, L., Zhou, Z. H., Liu, Z., et al. (2010) A novel intracellular protein delivery platform based on single-protein nanocapsules. *Nat. Nanotechnol.* 5, 48–53.

(18) Chou, T. C., and Talalay, P. (1984) Quantitative analysis of dose-effect relationships: the combined effects of multiple drugs or enzyme inhibitors. *Adv. Enzyme Regul.* 22, 27–55.

(19) Boyer, C., Huang, X., Whittaker, M. R., Bulmus, V., and Davis, T. P. (2011) An overview of protein-polymer particles. *Soft Matter* 7, 1599–1614.

(20) Chou, T. C. (2010) Drug combination studies and their synergy quantification using the Chou-Talalay method. *Cancer Res.* 70, 440–446.

(21) Holland, W., Chinn, D., Lara, P., Jr., Gandara, D., and Mack, P. (2014) Effects of AKT inhibition on HGF-mediated erlotinib resistance in non-small cell lung cancer cell lines. *J. Cancer Res. Clin. Oncol.* 1–12.

(22) Chou, T.-C. (2014) Frequently asked questions in drug combinations and the mass-action law-based answers. *Synergy* 1, 3–21.

(23) Templeton, A. C., Wuelfing, W. P., and Murray, R. W. (1999) Monolayer-protected cluster molecules. *Acc. Chem. Res.* 32, 27–36.

(24) Brust, M., Walker, M., Bethell, D., Schiffrin, D. J., and Whyman, R. (1994) Synthesis of thiol-derivatised gold nanoparticles in a two-phase Liquid-Liquid system. *J. Chem. Soc., Chem. Commun.*, 801–802.